

Modifying Fragility and Collective Motion in Polymer Melts with Nanoparticles

Francis W. Starr

Department of Physics, Wesleyan University, Middletown, Connecticut 06459, USA

Jack F. Douglas

Polymers Division, National Institute of Standards and Technology, Gaithersburg, Maryland 20899, USA

(Received 31 August 2010; published 15 March 2011)

We investigate the impact of nanoparticles (NP) on the fragility and cooperative stringlike motion in a model glass-forming polymer melt by molecular dynamics simulation. The NP cause significant changes to both the fragility and the average length of stringlike motion, where the effect depends on the NP-polymer interaction and NP concentration. We interpret these changes via the Adam-Gibbs (AG) theory, assuming the strings can be directly identified with the abstract “cooperatively rearranging regions” of AG. Our findings indicate that fragility is primarily a measure of the temperature dependence of the cooperativity of molecular motion.

DOI: [10.1103/PhysRevLett.106.115702](https://doi.org/10.1103/PhysRevLett.106.115702)

PACS numbers: 64.70.pj

The addition of a small concentration of nanoparticles (NP) to glass-forming (GF) polymer materials can lead to large property changes that are difficult to comprehend by extension of the effects of macroscopic filler additives. Depending on system details, changes may be rationalized by the large surface-to-volume ratio of the NP, chain bridging [1–3], or NP self-assembly into extended structures [4,5]. Changes in the glass transition temperature T_g have been particularly emphasized, and both experimental and theoretical studies indicate that attractive or repulsive (nonattractive) polymer-NP interactions tend to increase or decrease T_g , respectively. Correspondingly, the interfacial polymer layer around the NP shows a slowing down (increased T_g) or an acceleration of dynamics (decreased T_g), providing a molecular scale interpretation of the T_g changes [6–9].

Unfortunately, T_g changes provide only a limited characterization of how NP affect GF polymer melts. We also expect the T dependence of dynamical properties approaching T_g , or the “fragility” of glass formation [10], to be altered. Fragility changes have been argued for on theoretical grounds [11], based on the finding that changes in the molecular packing in the glass state ($T < T_g$) should also alter the fragility of glass formation. The NP we study should be particularly effective at modifying molecular scale packing and motion since their size is roughly commensurate with the nanoscale heterogeneity of fluids near T_g [12].

In this Letter, we address how polymer-NP interactions and NP concentration affect the fragility of glass formation, and how fragility relates to the extent and temperature dependence of cooperative motion. We demonstrate that the changes in the relaxation time τ can be related to changes in the average size L of the stringlike cooperative motion of monomers. The Adam-Gibbs (AG) theory [13]

predicts a specific relationship between the size of hypothetical “cooperatively rearranging regions” (CRR) and structural relaxation time. If L corresponds to the size of the CRR, we find that the AG relation holds for all concentrations ϕ and interaction types considered. Additionally, the AG theory predicts that fragility is sensitive to the T dependence of the size of CRR, and we confirm this relationship.

Our findings are based on equilibrium molecular dynamics simulations of a nanoparticle surrounded by a dense polymer melt, as well as simulations of a pure melt for comparison purposes. We utilize periodic boundary conditions so that our results represent an ideal, uniform dispersion of NP. The polymers are modeled by a well-studied bead-spring model [14], but with the cutoff distance between pairs extended to include attractive Lennard-Jones (LJ) interactions. All monomer pairs interact via a LJ potential, and bonded monomers along a chain are connected via a finitely extensible nonlinear elastic (FENE) spring potential. The NP consists of 356 Lennard-Jones particles bonded to form an icosahedral NP; the facet size of the NP roughly equals the equilibrium end-to-end distance for a chain of 20 monomers. Details of the simulation protocol and our model potentials can be found in the supplemental material [15] and in Ref. [8].

We simulate systems with 100, 200, or 400 chains of $M = 20$ monomers each (for totals of $N = 2000, 4000,$ and 8000 monomers) to address the effect of varying the NP volume fraction. Under constant pressure conditions, the addition of nanoparticles can give rise to a change in the overall melt density. A slight change in density can cause a significant change in the dynamic properties relative to the pure melt. In order to probe only changes caused by the interactions between the NP and the polymer melt, we have matched the density of monomers far from the NP with that of the pure polymer melt [8].

To quantify changes in the nanocomposite dynamics, we evaluate the effect of ϕ and the polymer-NP interactions on τ , measured from the relaxation of the coherent intermediate scattering function (see supplemental information [15]). The effects of interactions on τ and T_g for some ϕ were presented in Ref. [8]; here we provide additional simulation data and focus our analysis on fragility and cooperative motion. As expected, Fig. 1 shows that attractive polymer-NP interactions slow the relaxation (τ becomes larger), while nonattractive polymer-NP interactions give rise to an increased rate of relaxation (τ becomes smaller). The effect of ϕ is more clearly seen by rescaling τ by the value τ_{pure} in the pure melt, which shows that τ can be altered by a factor of more than an order of magnitude on cooling. The effect of the NP is more pronounced at low T .

We next examine how these changes in τ affect T_g and fragility. For reference, the inset of Fig. 1 confirms that T_g increases when there is attraction, and decreases with nonattractive interactions. To estimate T_g , we fit the data using the Vogel-Fulcher-Tammann (VFT) expression [10] $\tau \propto \exp(D/[T/T_0 - 1])$. T_0 is an extrapolated divergence T of τ , while D provides one measure of the fragility. We use the VFT fit to estimate T_g based on the condition that $\tau(T_g) = 100$ s (the canonical definition of the laboratory glass transition [10]), assuming that one time unit in standard LJ reduced units corresponds to 1 ps (reduced units defined in supplemental information [15]).

Since there is no single agreed upon measure of fragility, we consider several different measures to ensure consistency. First, as indicated above, the parameter D from a

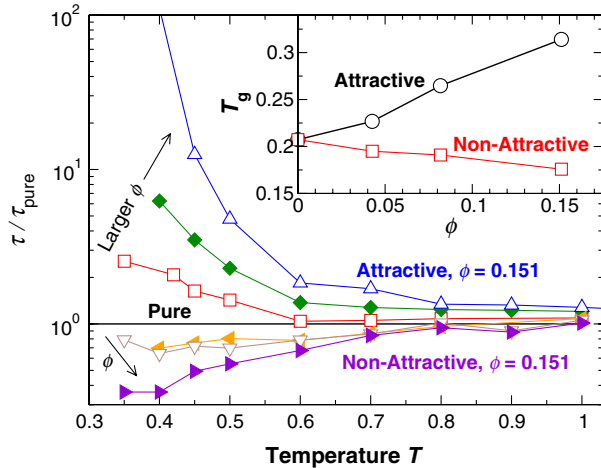


FIG. 1 (color online). Structural relaxation time τ as a function of T for each ϕ normalized by τ_{pure} for the pure melt. The inset shows the corresponding T_g as a function of concentration ϕ . Attractive interactions increase τ and T_g , while nonattractive interactions decrease τ and T_g . In both cases, the effect is more pronounced with increasing concentration. The concentrations are $\phi = 0.0426$ (red \square and orange \blacktriangleleft), 0.0817 (green \blacklozenge and brown \blacktriangledown) and 0.151 (blue \triangle and violet \blacktriangleright). The pure melt is indicated in black. The fits of the VFT relation to the data deviate by at most 0.5%.

VFT fit to τ is widely utilized; specifically, a larger value of D indicates a stronger (less fragile) GF fluid so that D^{-1} increases with increasing fragility. The most common definition of fragility is based on the T dependence of τ near T_g , namely [16],

$$m = \left. \frac{d(\ln\tau)}{d(T_g/T)} \right|_{T_g}. \quad (1)$$

For strong GF systems, the rate of change of τ with respect to T is smaller than that of fragile systems; hence m is larger for more fragile GF fluids. We estimate m using our VFT fit. Fragility can also be estimated by the ratios T_0/T_g or T_g/T_c . We estimate T_c using the power-law form $\tau \sim (T/T_c - 1)^{-\gamma}$ in an appropriate T range (see supplemental information [15] for fitting details). T_0/T_g and T_g/T_c are larger in more fragile systems [11].

We summarize the results for the various fragility metrics in Fig. 2(a), where we find that—for all definitions—attractive polymer-NP interactions lead to more fragile

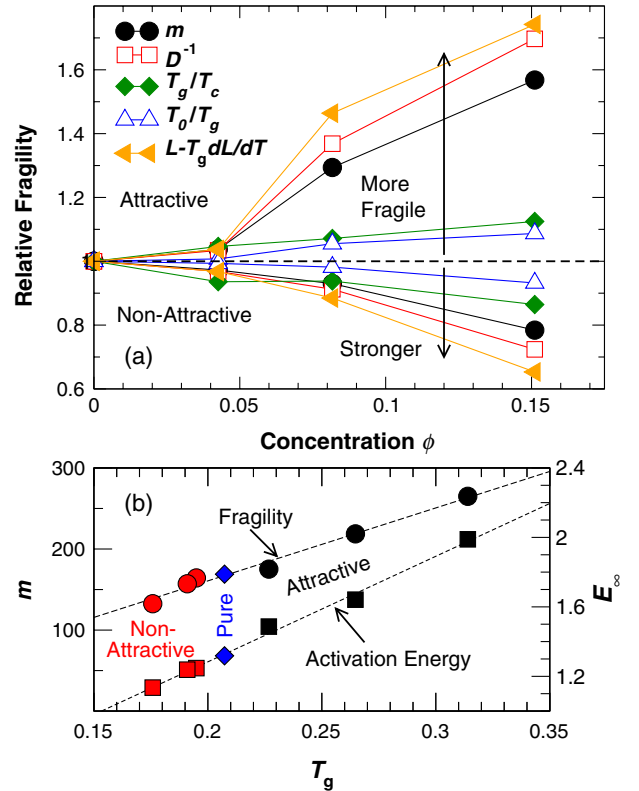


FIG. 2 (color online). (a) Fragility dependence on concentration ϕ relative to the pure melt. We consider five different measures of fragility, which are discussed in the text. All measures of fragility show the same qualitative trend: namely, the system with attractive polymer-NP interactions becomes more fragile, while the system with nonattractive interactions becomes less fragile (stronger). The last measure, related to the string length L , is discussed later in the text. (b) Demonstration of the proportionality between T_g and fragility m , as well as the high- T activation energy E_∞ . The different colors of symbols indicate the nature of the polymer-NP interactions.

glass formation as a function of ϕ ; conversely, nonattractive polymer-NP interactions lead to stronger glass formation. These changes in fragility mirror the changes in T_g (Fig. 1 inset). In particular, Fig. 2(b) shows that $m \propto T_g$, consistent with experimental trends in pure polymeric glass formers [17] and analytic calculations based on the entropy theory of glass formation [18]. Figure 2(b) also shows that the high- T activation energy E_∞ is roughly proportional to T_g . We discuss the implications of these scaling relationships below.

Our findings for fragility changes are consistent with experimental studies of polymer-NP systems. Bansal *et al.* [6] found that dispersions of NP having repulsive interactions caused T_g to decrease, accompanied by an appreciable broadening of the glass transition region, indicative of increased strength (decreased fragility) of glass formation. For fullerenes dispersed in polystyrene, Cabral and co-workers [19] reported behavior expected for attractive polymer-NP interactions, namely, an increase in T_g , accompanied by an increased fragility. For small ϕ , negligible changes in the fragility have been reported [20], also consistent with our small ϕ results. Our results are likely not applicable when the NP-polymer interactions are so strong that nonequilibrium effects (leading to “bound” polymer) [21] or phase separation dominates.

We next examine how the NP interactions impact the heterogeneity of molecular motions and how this relates to the observed changes in T_g and fragility. Both small-molecule and polymeric liquids exhibit pronounced spatial correlations in mobility, commonly referred to as “dynamical heterogeneity” [12]. In particular, the most mobile atoms or molecules tend to cluster on a time scale after the “breaking of the cage,” but before the primary relaxation τ . These clusters of mobile molecules can be further dissected into “strings” involving particles moving roughly colinearly [22]; these structures appear to be the most basic units of cooperative relaxation. The characteristic size of both the mobile-particle clusters and strings grow as a fluid is cooled toward T_g . Notably, the stringlike collective motion is not strongly correlated with chain connectivity [23], so it should not be confused with reptative motion.

We evaluate the string size $L(T)$ following the procedures developed in Ref. [22], which are slightly modified for the specific case of the bead-spring polymer we study, as discussed in Ref. [23]. Figure 3 shows L for all T and ϕ , where we compare systems by normalizing by the value of L of the pure melt. Given that L grows as τ grows on cooling, we expect that the attractive NP interactions (which increase τ relative to the pure melt) should cause L to increase relative to the pure melt, and vice versa for nonattractive NP interactions. Indeed, the variation of L is consistent with these expectations, and we conclude that the attractive NP interactions cause an increase in the degree of correlated molecular motion for fixed T , while nonattractive NP interactions cause a decrease in L .

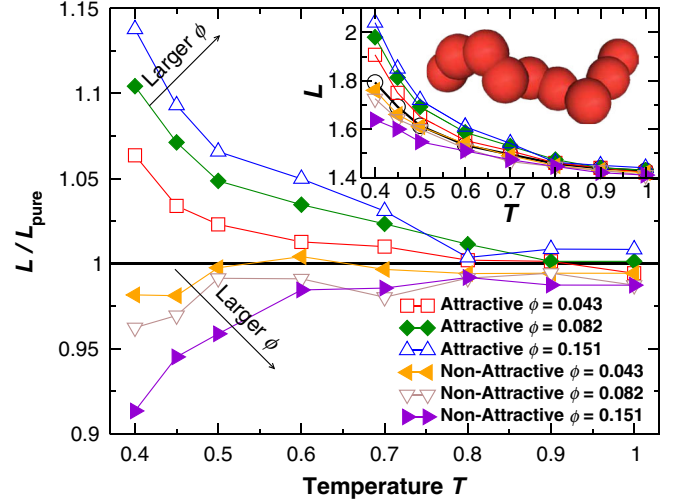


FIG. 3 (color online). T dependence of L for different ϕ normalized by L for the pure melt. Note the parallelism to Fig. 1. The inset also shows a snapshot of an example string of length, $L = 9$.

Note that the T dependence of L is qualitatively similar in all cases.

While the changes in L reflect the changes in τ for any given T , how does the T dependence of these changes compare? In other words, can L be used to predict the fragility changes in Fig. 2(a)? To answer this question, we are guided by AG theory, which proposes that relaxation in GF liquids is dominated by cooperatively rearranging regions (CRR). Specifically, AG argue that τ is related to the average number of particles z in the CRR by a generalized Arrhenius relation [24],

$$\tau = \tau_\infty \exp(zE_\infty/T). \quad (2)$$

For high T , cooperativity is minimal, so $z \approx 1$, and E_∞ (a constant) can be identified with the high- T activation energy of the fluid. Accordingly, the T -dependent activation energy $E(T) = z(T)E_\infty$ should govern the fragility.

The strings are a natural candidate to describe the abstract CRR of AG. Figure 4 shows that Eq. (2) with $z \propto L$ provides an excellent prediction for τ , consistent with identifying L with the CRR of AG [25]. Therefore, the non-Arrhenius behavior of τ can be viewed as a consequence of the increase in L on cooling. Accordingly, L must encode the fragility of glass formation. In particular, combining Eqs. (1) and (2) implies a direct relation between m and L ,

$$m = (E_\infty/T_g)[L(T_g) - T_g dL/dT|_{T_g}]. \quad (3)$$

Since E_∞ and T_g are proportional [Fig. 2(b)], the prefactor E_∞/T_g is roughly constant for all ϕ , and thus does not impact the nanocomposite fragility relative to the pure melt. Therefore, the fragility changes measured by m on adding NP should result from changes to L and TdL/dT at

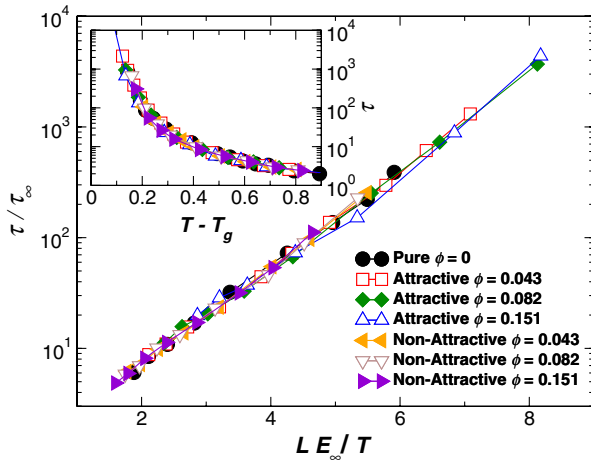


FIG. 4 (color online). Test of the AG relation [Eq. (2)] between the size of CRR and the structural relaxation time τ , assuming $z \propto L$. The main figure shows the data scaled by the fit parameters so that all data sets collapse to a master curve. τ_∞ is defined by Eq. (2), replacing z by L . The inset shows that τ can be collapsed by plotting as a function of $T - T_g$, a result of the proportionality of T_g and m [see Fig. 2(b)].

T_g . To test this, we extrapolate L to T_g by assuming consistency between Eq. (2) and the VFT expression. Figure 2(a) shows that $L - T_g dL/dT$ indeed accounts well for the observed changes in m . In particular, the contribution to Eq. (3) from $T_g dL/dT$ is 3 to 8 times larger than L , which ranges from 4.5 to 6.5 at T_g . The range for L is quantitatively consistent with Ref. [11], and qualitatively consistent with experimental evidence for weak sensitivity of fragility to the scale of cooperativity [26,27]. Hence, near T_g , fragility is primarily controlled by dL/dT , rather than L , consistent with Ref. [28]. Stated more plainly, fragility is primarily a measure of the rate of change (i.e., dL/dT) of the extent of cooperative motion.

The approximate proportionality between m and T_g observed in our system [Fig. 2(b)], and for many high molecular mass polymer materials [17], implies an important simplification. Specifically, since $m \sim 1/D$, the product DT_g should be nearly constant, and hence τ should be a nearly universal function of $(T - T_g)$. The inset to Fig. 4 shows that such a shift collapses all our nanocomposite data rather well; this alternate data reduction also indicates the consistency of our T_g extrapolation. However, we are careful to point out that the proportionality $m \propto T_g$ is not universal [29], and this trend can even be reversed in polyelectrolyte materials of interest in battery applications [18,30].

In summary, the addition of NP to a polymer melt can lead to significant changes in both T_g and fragility, which can be related to the cooperative stringlike motion. Our results support the identification of the strings with the abstract CRR of the AG theory, and complement tests of the entropy formulation of the AG theory [31].

- [1] J. B. Hooper and K. S. Schweizer, *Macromolecules* **38**, 8858 (2005); **39**, 5133 (2006).
- [2] D. Gersappe, *Phys. Rev. Lett.* **89**, 058301 (2002).
- [3] S. T. Knauer, J. F. Douglas, and F. W. Starr, *J. Polym. Sci., Part B: Polym. Phys.* **45**, 1882 (2007).
- [4] F. W. Starr, J. F. Douglas, and S. C. Glotzer, *J. Chem. Phys.* **119**, 1777 (2003).
- [5] P. Akcora *et al.*, *Nature Mater.* **8**, 354 (2009).
- [6] A. Bansal *et al.*, *Nature Mater.* **4**, 693 (2005).
- [7] J. A. Forrest and K. Dalnoki-Veress, *Adv. Colloid Interface Sci.* **94**, 167 (2001).
- [8] F. W. Starr, T. B. Schröder, and S. C. Glotzer, *Phys. Rev. E* **64**, 021802 (2001); *Macromolecules* **35**, 4481 (2002).
- [9] J. A. Torres, P. F. Nealey, and J. J. de Pablo, *Phys. Rev. Lett.* **85**, 3221 (2000).
- [10] C. A. Angell, *Science* **267**, 1924 (1995); K. Kunal *et al.*, *Macromolecules* **41**, 7232 (2008).
- [11] J. Dudowicz, K. F. Freed, and J. F. Douglas, *Adv. Chem. Phys.* **137**, 125 (2008).
- [12] M. D. Ediger, *Annu. Rev. Phys. Chem.* **51**, 99 (2000); R. Richert, *J. Phys. Condens. Matter* **14**, R703 (2002); C. Donati *et al.*, *Phys. Rev. E* **60**, 3107 (1999).
- [13] G. Adam and J. H. Gibbs, *J. Chem. Phys.* **43**, 139 (1965).
- [14] G. S. Grest and K. Kremer, *Phys. Rev. A* **33**, 3628 (1986).
- [15] See supplemental material at <http://link.aps.org/supplemental/10.1103/PhysRevLett.106.115702> for definitions of simulation units and the intermediate scattering function, as well as a description of fitting protocols.
- [16] C. A. Angell, *J. Non-Cryst. Solids* **73**, 1 (1985).
- [17] Q. Qin and G. B. McKenna, *J. Non-Cryst. Solids* **352**, 2977 (2006).
- [18] E. B. Stukalin, J. F. Douglas, and K. F. Freed, *J. Chem. Phys.* **131**, 114905 (2009).
- [19] H. C. Wong, A. Sanz, J. F. Douglas, and J. T. Cabral, *J. Mol. Liq.* **153**, 79 (2010).
- [20] H. Oh and P. F. Green, *Nature Mater.* **8**, 139 (2009).
- [21] S. E. Harton *et al.*, *Macromolecules* **43**, 3415 (2010).
- [22] C. Donati *et al.*, *Phys. Rev. Lett.* **80**, 2338 (1998).
- [23] M. Aichele *et al.*, *J. Chem. Phys.* **119**, 5290 (2003).
- [24] The original AG arguments do not discriminate between relaxation times associated with the mass, momentum, and energy diffusion processes. Since AG emphasize activated mass transport, it is natural to apply their arguments to a mass diffusion relaxation time. However, the decoupling relation between structural α relaxation τ and diffusivity implies that AG can also be applied to τ , but with a modified high temperature activation energy.
- [25] N. Giovambattista, S. V. Buldyrev, F. W. Starr, and H. E. Stanley, *Phys. Rev. Lett.* **90**, 085506 (2003).
- [26] L. Berthier *et al.*, *Science* **310**, 1797 (2005).
- [27] L. Hong, V. N. Novikov, and A. P. Sokolov, *J. Non-Cryst. Solids* (to be published).
- [28] J. F. Douglas, J. Dudowicz, and K. F. Freed, *J. Chem. Phys.* **125**, 144907 (2006).
- [29] V. N. Novikov and A. P. Sokolov, *Nature (London)* **431**, 961 (2004); A. P. Sokolov, V. N. Novikov, and Y. Ding, *J. Phys. Condens. Matter* **19**, 205116 (2007).
- [30] D. Fragiadakis, S. Dou, R. H. Colby, and J. Runt, *J. Chem. Phys.* **130**, 064907 (2009).
- [31] A. Scala *et al.*, *Nature (London)* **406**, 166 (2000); I. Saika-Voivod, P. H. Poole, and F. Scortino, *Nature (London)* **412**, 514 (2001); S. Sastry, *Nature (London)* **409**, 164 (2001).